Minimizing Edge Diffraction Using Modified Theory of Physical Optics (MTPO).

AsianubaIfeoma .B.[1*] and Okerulu Charles .I.[2]

[1]Dept. of Elect. /Elect. Eng. University of Port Harcourt, Rivers State Nigeria
[2]Dept. of Elect. /Elect. Eng. Federal Polytechnic Nekede, Owerri Imo State Nigeria

Abstract: *In this paper, minimizing edge diffraction in parabolic antenna for satellite communication has been achieved by deploying MTPOapproach. Edge Point Technique (EPT) and Stationery Point Method (SPM) were used by MTPO to model the edge diffraction and scattered fields, in order to reduce edge diffraction that manifested as side lobe radiations. Polar and rectangular plots were used to compare the results of both MTPO and PO (Physical Optics) approach. It was seen that edge diffraction appeared as side lobes that depends on antenna distance between the focus and reflecting surface. It was also seen from the result that MTPO considered two surfaces (perfectly conducting surface (PCS) and aperture), which gave reduced side lobe radiation as compared to the PO, which used only the PCS. The reduction in side lobes from MTPO and PO are 1dB, 2dB and 1dB respectively. When same rectangular and polar plots were used to compare MTPO and PO beamwidth,It was discovered that the beam width of MTPO is narrower than PO, but PO has a higher field strength than MTPO. The narrowness of MTPO beam width causes increase in directivity, SNR (signal to noise ratio) and efficiency. A parabolic antenna modelled with minimized edge diffraction finds application in satellite communication and outdoor digital signal reception at home.*

Keywords: *MTPO, PO, Edge Diffraction, Parabolic Antenna, Detour Parameter.*

I.   Introduction

Parabolic antennas are mainlymade up ofthe feed at its focus and the reflector. The reflector is a surface made of metal and constructed into a parabolic form with the rim, circular in shape. The diameter of the antenna is determined by its shape. While the feed antenna at the focus may be low gain, coaxial cable or hollow waveguide is used to provide link between feed antenna and radio frequency (RF) transceiver equipment. In order not to receive noise from the back of the parabolic antenna. The focus antenna beam width must match the focal length to diameter ratio(f/D) of the parabolic antenna, if this ratio is not achieved, over illuminated or under illuminated reflector antenna may result. The antenna efficiency depends largely on dish diameter, f/D and how effective dish illumination is done by the antenna.

The merits of parabolic antenna include:
i.   They are easy to fabricate.
  ii.   Small gain antenna and feed can be employed to achieve high gain.
  iii. Spill over and minor radiation are minimal.
  iv.   Long distance communication system is cost effective since complete transceiver can be located at the focus.
  v.   The size of the beam is dependent on the movement of reflecting surface **[1].**

Parabolic antenna is a reflector antenna with the potentials of holding back or radiating most of electromagnetic energy, over its aperture into a focal plane or far field for communication.Applications of parabolic antennas can be found in weaponry, radars, home satellite television receiver, spacecraft, radio astronomy and satellite communication **[2].**

The three main mechanism for propagation of electromagnetic wave are reflection, diffraction and scattering. Reflection dominates indoor propagation but becomes inefficient for outdoor communication due to reduction of signal strength as a result of multiple transmission. Scattering on the other hand is not significant both for indoor and outdoor applications due to reduction in power level, but scattering is employed where receiver or transmitter is located in highly cluttered environment. Finally, diffraction is simply bending of electromagnetic wave around corners to reach areas, which are otherwise not reachable (shadowed region). It is less significant for indoor application but find more use for outdoor communication, it is used where signal transmission through the building is virtually impossible **[3].**

The objective of this paper, is to model and reduce edge diffraction in parabolic antenna. MTPO is used to model scattering in parabolic reflector, cylindrical and parabolic reflectors will be compared mathematically,

---

followed by comparison between MTPO and PO using rectangular and polar plots. The method adopted in this work include the following:

i. Formulation of the MTPO, to model the scattered fields of the parabolic reflector was considered.
ii. Evaluation of the scattered fields using Edge point Technique (EPT) and Stationery Point Method (SPM).
iii. Non uniform solutions were converted to uniform solution using Detour parameter.
iv. The fundamental equation of the total scattered fields of the parabolic reflector was obtained.
v. Simulations to show reduction in edge diffraction problem and to show the narrower beam width of MTPO.

II. Review Of Related Works

[4]Studied the effect of illumination at the aperture and the rolling effect at the edge for antenna design (parabolic reflector). This was because parabolic dishes have large physical dimension with respect to the wavelength. The far field antenna characteristics were determined by using GO (Geometrical Optics), PO, Aperture Integration (AI) and GTD (Geometrical Theory of Diffraction), which were called high frequency electromagnetic wave scattering techniques. MOM (Moment of Methods), FEM (Finite Element Method) and FDM (Finite Difference Method) were some direct numerical techniques used for non-canonical structures. The hard numerical convergence problem was created because of computational instabilities, complexity of some cavity or aperture geometries. The work applied 2D ARM (Analytical Regularization Method) to a structure with cylindrical parabolic shape which diffracted E-polarized wave to realize reflector antenna with correct analysis that was parametric in nature. The result obtained shows that edge diffraction is the main problem of parabolic reflector but can be minimized by decreasing the aperture illumination on the edges of the reflector. Also, edge rolling technique reduced edge diffraction regardless of aperture illumination, achieved by circularly rolling backward the dish's edge at different diameter.

[5] Analysed the compact range reflector with serrated edge. The work developed and applied an analytical tool with the purpose of developing an improved serrated design. Computer simulation of compact range scattering and result measurement were carried out. The computer model employed four basic steps to analyse a compact range reflector, which were perimeter generation, integration patch determination, surface current determination and field evaluation at observation points. The result showed that to mitigate edge diffraction effect, serrated treatment was used and geometry of edge, slope of edge and electrical size were examined. Edge geometry was used to produce smooth transition between the reflecting surface of the antenna and free spaceat the tip of serrations, Edge slope reduced the extraneous energy in the quiet zone and diffraction cone defined the orientation and direction in which the edge extends from the main body of the reflector. Finally, for electrical size, diffraction control became better with larger edge treatment and for a given performance level, the overall physical size of a reflector should be minimized.

[6]Studied reflector antennas using induced current. Several analytical techniques have been employed to calculate diffraction pattern of reflector antenna such as AI, GTD, GTD+GO, UAT (Uniform Asymptotic Theory), UTD (Uniform Theory of Diffraction) and ECM (Equivalent Current Method). But each and every one of them comes with its own merits and demerits, AI was used for main beam and near inside lobes while GTD+GO was used to predict the far out side and back lobes. GTD had shortcoming of predicting singular value in the region of transition nearshadow boundaries of GO incident and reflection but cannot give information about diffracted field adjacent to the caustic region. The work used Induced Current Analysis of Reflector Antenna (ICARA) software to predict the behaviour of reflector antenna using the PO method. The result obtained shows that PO approximation was used for objects with large electrical size, small local curvature and provided adequate estimation of current with less computational cost. For single and dual reflector antenna design, ICARA software provided a user friendly graphical interface and was used for both procedure analysis and to show graphical results.

[7]Studied modern high frequency methods for solving electromagnetic scattering problem. The work reviewed important high frequency techniques. High frequency method are classified based on current and ray, current based examples include: PO, PTD and ILDC (incremental Length Diffraction Coefficient) which permitted reflected and diffracted fields to be calculated using different mathematical techniques. While ray based method examples include UTD, GO, GTD and UAT. MOM, FEM and FDTD (Finite Difference Time Domain) methods are efficient method developed to simulate electromagnetic field with high accuracy and speed. NSDP (Numerical Steepest descent Path) was employed to calculate high frequency scattered from PO and ILDC. PO scattered fields were represented as surface integral whereas the field due to diffracted wave because of ILDC technique was represented as line integral. The result obtained shows that NSDP demonstrated error controllable accuracy and workload that is not dependent on frequency. Also, NSDP improved its accuracy by around two digits, when the working frequency is not extremely large.

[8] Studied the rigorous expression for the equivalent edge currentsby using MTPO axioms and high frequency asymptotic solution of the half plane problem. The edge current was expressed in terms of scattered and incident rays.The result showedthat MTPO gave the exact diffracted waves for scattered problem by

conducting bodies,using its three axioms to solve the problem of PO's in correct edge contributions of the scattered integral. Also, the function of the corner diffracted field was analogous to the edge diffracted wave with a dimension difference.

[9] Studied radiation from parabolic type radio link antenna. The work constructed scattering surface integral of MTPO and also field scattering from parabolic reflector with perfect electric surface. The method used was MTPO to calculate the scattered field from perfectly conducting body. It used three axioms to construct the scattered field and employed stationery point method (SPM) &edge point technique (EPT) to asymptotically evaluate reflected, transmitted and edge diffracted field. The result showed that spherical coordinates solved wrong value problem, when MTPO scattered field was combined with edge diffraction. Asymptotic evaluation of the integral gave GO fields (reflected and transmitted) and edge diffracted fields.

III.   Methodology

MTPO Formulation
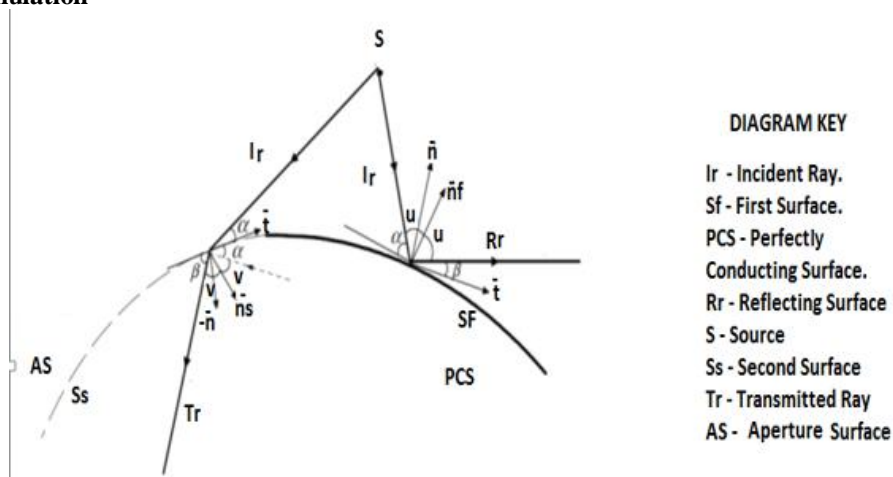
Fig.1 Geometry of scattering field in MTPO.

MTPOis based on two surfaces S_F and S_S as shown in fig 1. The surface current for S_F ($\vec{J}es$), equivalent surface current for S_S ($\vec{J}es$) and magnetic current density ($\vec{j}ms$) are equal to the MTPO normal vectors ($\vec{n}_F$ and $\vec{n}_S$) of the concerned surfaces ($S_F + S_S$), the electric and magnetic fields.

$$\vec{J}es = \vec{n}f \times \vec{H}tot|S_F \qquad (1)$$
$$\vec{J}es = \vec{n}s \times \vec{H}inc|S_S \qquad (2)$$
$$\vec{j}ms = -\vec{n}s \times \vec{E}inc|S_S \qquad (3)$$

Where
Einc =Incident electric field.
$\vec{H}$inc=Incident magnetic field.
$\vec{H}$tot=Total magnetic field.
$\vec{n}_F$ and $\vec{n}_S$= MTPO unit vector for first and second surfaces respectively.
β = the reflection angle that relied on the surface ($S_F + S_S$) coordinates.
$S_F$and S_S= first surface (Reflector surface) and second surface (Aperture Surface).
$\vec{J}es$ = Surface current for S_F.
$\vec{J}es$ = Equivalent surface current for S_S.
$\vec{J}ms$ = Magnetic current density.
[10]From the third axioms, MTPO gave the unit vector for S_F and S_S as shown below

$$\vec{n}_F = \cos (u+\alpha)\ \vec{t} + \sin (u+\alpha)\vec{n} \qquad (4)$$
$$\vec{n}_S = \cos (v+\alpha)\vec{t} - \sin (v+\alpha)\vec{n} \qquad (5)$$

Where α = Angle of incidence.
$\vec{n}$ = Surface normal unit vector.
$\vec{t}$ = Actual tangential of the surface.

The boundary conditions of equations 1, 2 and 3 are evaluated using the new unit vector where $u = v = \frac{\pi}{2} - \frac{\alpha+\beta}{2}$ (6)

The total scattered electric field$\vec{E}$totand the total scattered magnetic field $\vec{H}$tot can be found to be

$$\vec{E}tot = \vec{E}incsc + \vec{E}refsc \qquad (7)$$
$$\vec{H}tot = \vec{H}incsc + \vec{H}refsc \qquad (8)$$

Where

$\vec{E}incsc$ = Incident scattered electric field.

$\vec{E}refsc$ = Reflected scattered electric field.

$\vec{H}incsc$ = Incident scattered magnetic field.

$\vec{H}refsc$ = Reflected scattered magnetic field.

$\vec{E}incsc = -\frac{j\omega\mu_o}{4\pi} \iint_{S_s} \vec{n}\, s \; x \overrightarrow{H}inc|s_s \frac{e^{-jkR_2}}{R_2} ds' + \iint_{S_s} \nabla x\, (\vec{n}s\, x\vec{E}inc|s_s \frac{e^{-jkR_2}}{R_2}\;)\, ds'$ (9)

$\vec{E}refsc = -\frac{j\omega\mu_o}{4\pi} \iint_{S_f} \vec{n}f \; x\overrightarrow{H}tot|s_f \frac{e^{-jkR_1}}{R_1}\, ds'$ (10)

$\vec{H}refsc = \frac{1}{4\pi} \iint_{S_f} \nabla x\, (\vec{n}f \; x\; \overrightarrow{H}tot|s_f \frac{e^{-jkR_1}}{R_1})\, ds'$ (11)

$\vec{H}incsc = \frac{1}{4\pi} \iint_{S_s} \nabla x\, (\vec{n}s \; x\; \overrightarrow{H}inc|s_s \frac{e^{-jkR_2}}{R_2})\, ds' + \frac{J\omega\epsilon}{4\pi} \iint_{Ss} \quad \vec{n}s \; x\vec{E}inc|s_s \frac{e^{-jkR_2}}{R_2} ds'$ (12)

The magnetic and electric fields in the far field scattering are all gotten from $\vec{E}s \cong -J\omega\vec{A}$. But $\vec{A} = \frac{\mu_0}{4\pi} \iint_{S'}\, \vec{J}Gds'$ and $G = \frac{e^{-jkR}}{R}$, where $\vec{A}$ = Magnetic Vector Potential,ω = angular frequency, $\vec{E}s$ = Scattered Electric Field, μ_o = free space permeability, G = free space Green function and R = distance between source and observation point **[11].**
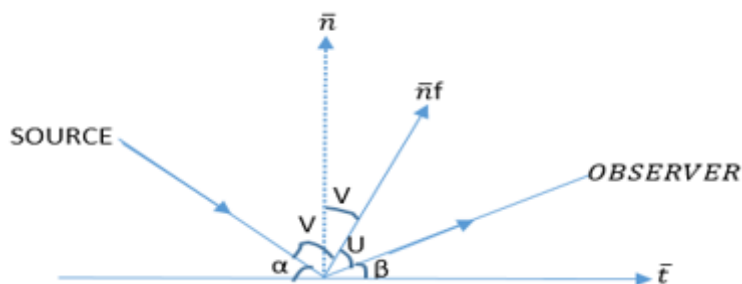

Fig.2 Scattered field when viewed from the edge

Parabolic Reflector Scattering

The incident electric field is given by **[12]** as

$\vec{E}inc = \vec{e}zE_O \frac{e^{-jk\rho}}{\sqrt{k\rho}}$ (13)

Where; $E_O = e^{j(\frac{\pi}{4})} \frac{\omega\mu_0 I_0}{2\sqrt{2\pi}}$

$\vec{e}z$ = Incident wave is z polarized

E_o = Complex amplitude factor

I_o = Source Current.

μ_0 = Free Space Permeability.

ω = Angular Frequency.

$\vec{H}inc = -\vec{e}\varphi \frac{Eo}{Zo} \frac{e^{-jk\rho}}{\sqrt{k\rho}}$ (14)

equation(14) was obtained from $\nabla\, x\, \vec{E}inc = j\omega\mu o\vec{H}inc$ but $\vec{H}inc = \frac{1}{Z_o}\hat{k} \; x\; \vec{E}inc$ as suggested **[12]** where;$\vec{E}inc = \vec{e}zE_O \frac{e^{-jk\rho}}{\sqrt{k\rho}}$,$Z_o = \sqrt{\frac{\mu_O}{\varepsilon_0}}$ and $k = \omega\sqrt{\mu_o\varepsilon_o}$.

Z_o = Free space impedance

k = Wave number in the free space

P = Distance between the source and reflector.

$\hat{k}$ = shows incident wave direction.

ε_o = Free space permittivity.

For perfectly conducting surfaces,$\vec{n}f \; x\; (\vec{E}incx\vec{E}ref) = 0$ and reflection is in the opposite direction to ρ, $\vec{H}ref = \vec{H}inc$ and $\vec{H}tot = 2\vec{H}inc$ equations can be found. **[13]**Usedcylindrical coordinate components in the form of normal and tangential vectors as formulated below

$\vec{n} = -\cos\frac{\varphi'}{2} \vec{e}\rho + \sin\frac{\varphi'}{2} \vec{e}\varphi$ (15)

$\vec{t} = \sin\frac{\varphi'}{2} \vec{e}\rho + \cos\frac{\varphi'}{2} \vec{e}\varphi$ (16)

According to fig.2, point vector can be shown in terms of $\vec{n}$and$\vec{t}$.

$\vec{n}f = \sin v \vec{t} + \cos v \vec{n}$ (17)

Substituting equations 15 and 16 into equation 17 gave the expressions below according to **[14]**

$\vec{n}f = -\sin\left(\frac{\alpha-\beta}{2}\right)\vec{e}\varphi + \cos\left(\frac{\alpha-\beta}{2}\right)\vec{e}\rho$ (18)

$\vec{n}s = \sin\left(\frac{\alpha+\beta}{2}\right)\vec{e}\varphi + \cos\left(\frac{\alpha+\beta}{2}\right)\vec{e}\rho$

Green function

$\int_{z=-\infty}^{\infty}\frac{e^{-jkR_1}}{R_1}dz^1 = \int_{z'=\infty}^{\infty}\frac{1}{2j}\int_{\xi=-\infty}^{\infty}Ho^{(2)}(\sqrt{(k^2-\xi^2\rho_1)}e^{-i\xi(z-z')}d\xi dz^1.$ (19)

[15] and **[16]** provided the identity to solve the scattering integral

$\int_{z'=-\infty}^{\infty}e^{i\xi z'}dz^1 = 2\pi\delta(\xi)$ (20)

Green function was simplified using equation 21

$\int_{z=-\infty}^{\infty}\frac{e^{-jkR1}}{R1}dz^1 = \frac{\pi}{j}Ho^{(2)}(k\rho_1)$ (21)

Where ξ = detour parameter and Ho^2 = Hankel function of second order.

[17] Provided Debye asymptotic expansion of Hankel function

$Ho^2(Kv) \approx \sqrt{\frac{2}{\pi}}\frac{e^{-jkv+j(\frac{\pi}{4})}}{\sqrt{kv}}$ (22)

Scattered field is the combination of reflected scattered electric field ($\vec{E}refsc$) and incident scattered electric field ($\vec{E}incsc$), equation 10 is multiplied with equation 21 gives;

$\vec{E}refsc = -\frac{\omega\mu_0}{4}\int_{z'=-\infty}^{\infty}\int_{-\varphi_o}^{\varphi_o}\vec{n}f \times \vec{H}tot|s_s\frac{\rho'}{\cos(\frac{\varphi'}{2})}\left(\sqrt{\frac{2}{\pi}}\frac{e^{-jkR+j(\frac{\pi}{4})}}{\sqrt{kR}}\right)d\varphi$

Substituting equation 18 for $\vec{n}f$ and equation 14 for $\vec{H}tot = 2x\vec{H}inc$ gives the below equation

$\vec{E}refsc = -\vec{e}z\frac{kE_oe^{j\frac{\pi}{4}}}{\sqrt{2\pi}}\int_{-\varphi_0}^{\varphi_o}\frac{\rho'}{\cos(\frac{\varphi'}{2})}\frac{e^{-jkR}}{\sqrt{kR}}\sin\left(\frac{\alpha-\beta}{2}\right)\frac{e^{-jkp}}{\sqrt{kp}}d\varphi$ (23)

For $\vec{E}incsc$, equation 9 is multiplied with equation 21 to give

$\vec{E}incsc = -\frac{\omega\mu_0}{4}\int_{z'=-\infty}^{\infty}\int_{-\varphi_o}^{\varphi_o}\vec{n}s \times \vec{H}inc|s_s\frac{\rho'}{\cos(\frac{\varphi'}{2})}\left(\sqrt{\frac{2}{\pi}}\frac{e^{-jkR+j(\frac{\pi}{4})}}{\sqrt{kR}}\right)dz'd\varphi + \frac{1}{4}\int_{z'=-\infty}^{\infty}\int_{-\varphi_o}^{\varphi_o}\nabla(\vec{n}s \times \vec{E}inc|s_s\frac{\rho'}{\cos(\frac{\varphi'}{2})}$

$\left(\sqrt{\frac{2}{\pi}}\frac{e^{-jkR+j(\frac{\pi}{4})}}{\sqrt{kR}}\right)dz'd\varphi.$

Substituting equation 18 for $\vec{n}s$, equation 14 for $\vec{H}inc$ and equation 13 for $\vec{E}inc$ gives equation 24

$\vec{E}incsc = \vec{e}z\frac{E_oke^{j\frac{\pi}{4}}}{\sqrt{2\pi}}\int_{-\varphi_0}^{\varphi_o}\frac{\rho'}{\cos(\frac{\varphi'}{2})}\frac{e^{-jkR}}{\sqrt{kR}}\cos\left(\frac{\alpha+\beta}{2}\right)\frac{e^{-jkp}}{\sqrt{kp}}d\varphi'$ (24)

Combining equations 23 and 24 gives 25

$\vec{E}sca = \vec{e}zE_o\left(\frac{e^{-jkp}}{\sqrt{kp}} + \frac{kE_oe^{j\frac{\pi}{4}}}{\sqrt{2\pi}}\right)\int_{-\varphi_o}^{\varphi_0}\left(\cos\left(\frac{\alpha+\beta}{2}\right) - \sin\left(\frac{\alpha-\beta}{2}\right)\right)\frac{e^{-jk\rho'}}{\sqrt{k\rho'}}\frac{e^{-jkR}}{\sqrt{kR}}\frac{\rho'}{\cos(\frac{\varphi'}{2})}d\varphi$ (25)

Evaluation of scattered integral using Edge Point Technique and Stationery Point Method.

[12] employed g (φ) and f (φ') in asymptotic evaluation of the scattering integral. Where g (φ) is the phase function, f (φ') is the amplitude function and e^{-jkl} is the phase delay factor. The phase and magnitude were gotten due to series of operations

g (φ) = R + ρ' (26)

f (φ') = $\frac{e^{i(\frac{\pi}{4})}Eo}{\sqrt{2\pi}}\sqrt{\frac{I_o}{I}}$ (27)

$\vec{E}refsca$ = Reflected scattered electric field and $\vec{E}transca$ = Transmitted scattered electric field are formulated as shown below

$\vec{E}refsca = \vec{e}zEo\frac{e^{-jklo}}{\sqrt{klo}}e^{-jkl}$ (28)

$\vec{E}transca = \vec{e}zEo\frac{e^{-ik\rho}}{\sqrt{k\rho}}$ (29)
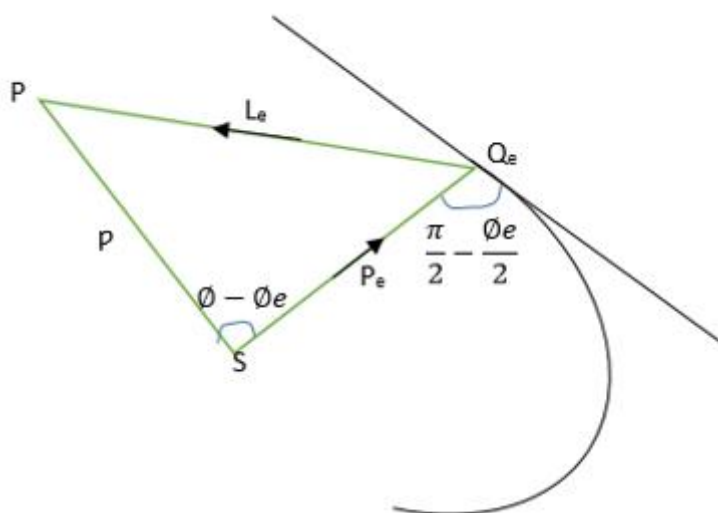

Fig.3 Edge diffraction originating from parabolic reflector

Edge point technique was used by **[17]** and the expression is

$$\vec{E}diff = \vec{e}z \frac{Eoe^{-j(\frac{\pi}{4})}}{k2\sqrt{2\pi}} \left(\frac{1}{\sin\frac{\beta e-\alpha e}{2}} - \frac{1}{\cos\frac{\beta e+\alpha e}{2}}\right) \frac{e^{-jk(\rho e + Ie)}}{\sqrt{\rho ele}} \qquad (30)$$

But $E_o = e^{i(\frac{\pi}{4})} \frac{\omega\mu_o I_o}{2\sqrt{2\pi}}$

Combining equation 30 and E_o gives

$$\vec{E}diff = \vec{e}z \frac{ZoIo}{8\pi} \left(\frac{1}{\sin\frac{\beta e-\alpha e}{2}} - \frac{1}{\cos\frac{\beta e+\alpha e}{2}}\right) \frac{e^{-jk(\rho e + Ie)}}{\sqrt{\rho ele}} \qquad (31)$$

Where $\vec{E}diff$ = Edge diffracted field

[17] Obtained the result from perfectly electric conducting cylindrical reflector as

$$\vec{E}diff = \vec{e}z \frac{ZoIo}{8\pi} \left(\frac{1}{\sin\frac{\beta e-\alpha e}{2}} - \frac{1}{\cos\frac{\beta e+\alpha e}{2}}\right) \frac{e^{-jk(l_0 + l_1)}}{\sqrt{l_0 l_1}} \qquad (32)$$

The result found for both cylindrical and parabolic surface as shown in equations 31 and 32 are coherent, since both terms P_e and l_e for parabolic reflector resembles l_o and l_1 for cylindrical reflector.

Diffraction coefficient D (φo) is gotten from $\vec{E}diff$

$$D (\varphi o) = \frac{e^{-j(\frac{\pi}{4})}}{2\sqrt{2\pi}} \left(\frac{1}{\sin\frac{\beta e-\alpha e,\varphi o}{2}} - \frac{1}{\cos\frac{\beta e+\alpha e,\varphi o}{2}}\right) \qquad (33)$$

Where $(-\varphi o)$ is diffraction coefficient for the other edge

$$D (-\varphi o) = \frac{e^{-j(\frac{\pi}{4})}}{2\sqrt{2\pi}} \left(\frac{1}{\sin\frac{\beta e-\alpha e,-\varphi o}{2}} - \frac{1}{\cos\frac{\beta e+\alpha e,-\varphi o}{2}}\right) \qquad (34)$$

Therefore the total diffracted field is

$$\vec{E}diff = \vec{e}zEo\frac{e^{-jk(\rho e + le)}}{k\sqrt{\rho ele}} (D (\varphi o) - D (-\varphi o)) \qquad (35)$$

Conversion of Non-uniform solution to Uniform solution using Detour Parameter

[18] Employed detour parameter (ξ) to remove these uncertainties making it possible for values that are uniform to be obtained since the denominator with sinusoidal factor has to be removed. The result may lead to infinity for some values. By using this trigonometry identity $1 = 2Sin^2\frac{x}{2} + Cosx$, diffracted field at the edge point (Q_e)can be found to be

$$\vec{E}diff = \vec{e}zEo\frac{e^{-j(\frac{\pi}{4})}}{2\sqrt{2\pi}} \frac{e^{-jk(\rho e + le)}}{k\sqrt{\rho ele}} \left(\frac{e^{(2Sin^2\frac{\beta e-\alpha e}{2} + Cos(\beta e-\alpha e)}}{Sin\frac{\beta e-\alpha e}{2}} - \frac{e^{(2cos^2\frac{\beta e+\alpha e}{2} - Cos(\beta e+\alpha e)}}{Cos\frac{\beta e+\alpha e}{2}}\right) \quad (36)$$

Since $\vec{E}diff = \vec{E}incdiff + \vec{E}refdiff$

$$\vec{E}incdiff = \vec{e}zEoe^{-jk\rho e} \frac{e^{-jkle}}{\sqrt{kle}} \left(\frac{e^{-j(\frac{\pi}{4})} e^{-jk\rho e} 2Sin^2\frac{\beta e-\alpha e}{2}}{2\sqrt{\pi}\sqrt{2k\rho e} \sin\frac{\beta e-\alpha e}{2}}\right)e^{\cos(\beta e-\alpha e)} \qquad (37)$$

$$\vec{\text{E}}refdiff = \vec{e}zEoe^{-jk\rho e}\frac{e^{-jkle}}{\sqrt{kle}} \left(\frac{e^{-j\left(\frac{\pi}{4}\right)} e^{-jk\rho e} 2cos^2 \frac{\beta e+\alpha e}{2}}{2\sqrt{\pi}\sqrt{2k\rho e} \, cos\frac{\beta e+\alpha e}{2}} \right)e^{\cos(\beta e+\alpha e)} \tag{38}$$

The incident and reflected field due to detour parameter (ξ) value

$$\xi_{\text{inc}} =\sqrt{2k\rho e} \, \text{Sin} \left(\frac{\beta e-\alpha e}{2}\right) \tag{39}$$

$$\xi_{\text{ref}}=\sqrt{2k\rho e} \, \text{Cos} \left(\frac{\beta e+\alpha e}{2}\right) \tag{40}$$

[19]Employed this integral as shown below

$$\hat{f}(\xi inc) =\frac{e^{-j(\xi inc^2 +\frac{\pi}{4})}}{2\sqrt{\pi} \, \xi inc} \tag{41}$$

$$\hat{f}(\xi ref) =\frac{e^{-j(\xi ref^2 +\frac{\pi}{4})}}{2\sqrt{\pi} \, \xi ref} \tag{42}$$

The uniform diffracted field at point (φo) is given by

$$\vec{\text{E}}diff = \vec{e}z \frac{Eoe^{-jk(pe+le)}}{\sqrt{k}le} f(\xi inc)e^{\text{Cos}(\beta e-\alpha e)} - f(\xi ref) \, e^{\cos(\beta e+\alpha e)} \tag{43}$$

The Total Scattered Field of Parabolic Reflector

Since singularities have been eliminated using detour parameter. The total scattered electric field is as shown equations 444 and 45

$$\vec{\text{TE}}sca = \vec{\text{E}}ref + \vec{\text{E}}diff(\varphi o)+ \vec{\text{E}}diff(-\varphi o) \tag{44}$$

$$\vec{\text{TE}}sca=\vec{e}zEo\frac{e^{-jklo}}{\sqrt{k}lo}e^{-jkl}+\vec{e}z \frac{Eoe^{-jk(pe+le)}}{\sqrt{k}le} f(\xi inc)e^{\text{Cos}(\beta e-\alpha e)} - f(\xi ref) \, e^{\cos(\beta e+\alpha e)}$$

$$+\vec{e}z \frac{Eoe^{-jk(pe+le)}}{\sqrt{k}le} f(\xi inc)e^{\text{Cos}(\beta e-\alpha e(-\varphi o))} - f(\xi ref) \, e^{\cos(\beta e+\alpha e(-\varphi o))}. \tag{45}$$

Equation 45 is the fundamental equation used to obtain parabolic reflector total scattered field.

IV.   Result And Discussion

The total scattered field of a parabolic reflector is analysed between $-\varphi_{o \; and}\varphi_o$ using polar and rectangular plots, the plots are produced by Mathlab. Polar plot shows the radiation pattern of both MTPO and PO while Rectangular plot gives a more detailed radiation pattern of main, side and back lobes for both MTPO and PO respectively. The rectangular plot makes it possible for calculation of the values of main lobes and side lobes in dB to be obtained and the formula, $10\log_{10}P$ allows the conversion of amplitude value to dB scale.

CASE 1:
The reflected field is numerically plotted using equation 28 with the following values $\varphi =[^{-\pi}/_2, 0.01, ^{\pi}/_2]$, d = 0.1m and n=4.The polar and rectangular plots are shown below
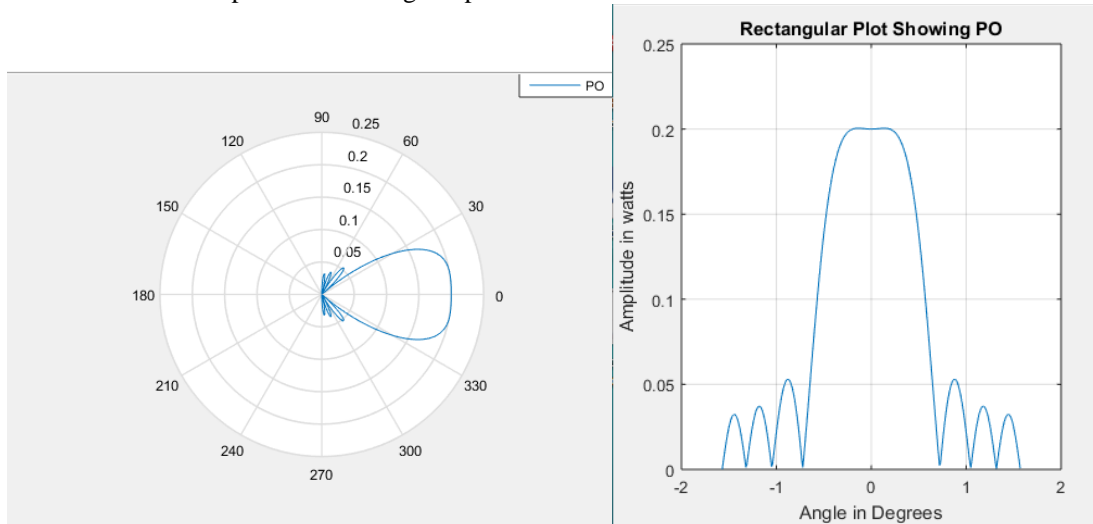

Fig.4 Reflected field due to PO using polar plot   Fig.5 Rectangular plot of PO

From the plot, the main lobe has high field strength with a lot of side lobes but no back lobe. The high field strength and no back lobe are of economic importance, since it is always the desire of antenna designer for efficient satellite communication. But, it is important to note that side lobes waste power and causes interference.

Table 1 Conversion of amplitude (w) to dB for main and side lobes of PO

S/N	LOBE	AMPLITUDE VALUE OF PO (WATTS)	PO IN dB
1	Main Lobe	0.200	-7
2	First Side Lobe	0.055	-13
3	Second Side Lobe	0.038	-14
4	Third Side Lobe	0.030	-15

From table 1, the main lobe is -7dB while that of side lobes are -13dB,-14dB and -15dB respectively. Which shows that the main lobe has a high field strength of -7dB but it has a problem of interference in unwanted direction due to side lobes.

CASE 2:
For MTPO, equation 45 is plotted using same value as in the case of PO. The total scattered field is plotted and the polar &rectangular plots of MTPO are shown below
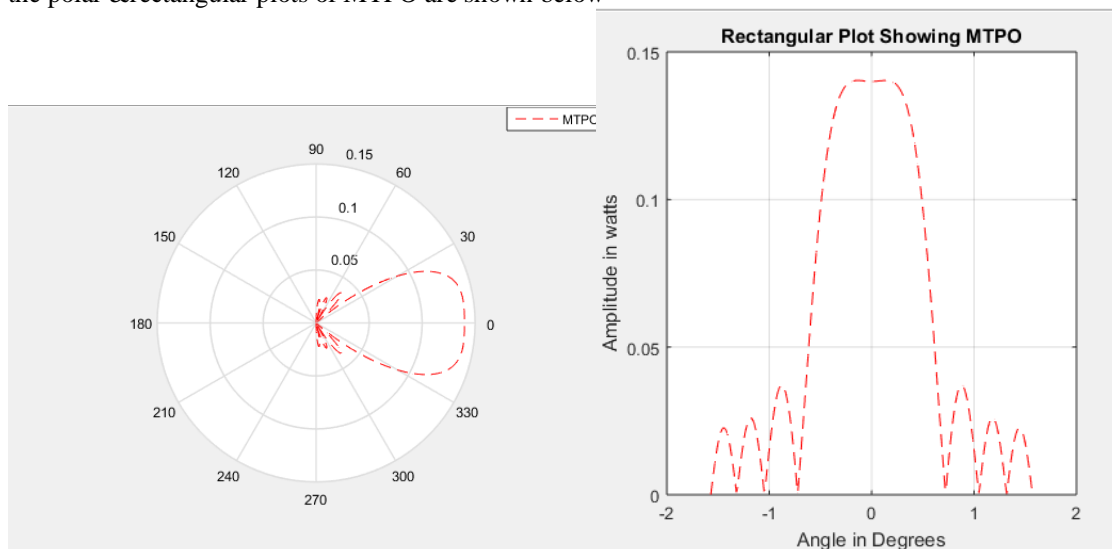

Fig.6 Total Scattered field due to MTPO   Fig.7 Rectangular Plot of MTPO

Using Polar plot
From the plot, the field strength of main lobe is reduced compared to that of PO and there is no back lobe, the side lobes of MTPO are reduced compared to PO. Because of the reduction in side lobe level, power wastage and interference are reduced.
From table 2, main lobe has a reduced field strength of -9dB while side lobes have -14dB,-16dB and -16dB as their values. The main lobe has a reduced field strength with reduced side lobes.

Table 2 Conversion of amplitude (w) to dB for main and side lobes of MTPO

S/N	LOBE	AMPLITUDE VALUE OF MTPO (WATTS)	MTPO IN dB
1	Main Lobe	0.1410	-9
2	First Side Lobe	0.0365	-14
3	Second Side Lobe	0.0269	-16
4	Third Side Lobe	0.0234	-16

CASE 3:
MTPO and PO are compared using the plots(polar and rectangular). From the plot, MTPO has minimized side lobe radiations than PO because of addition of aperture surface (second surface). This enabled edge diffraction to be calculated and reduced main lobe was because of distance (d) which is directly proportional to the main and side lobes. The distance (d) referred to here is the one between the focus antenna and the reflecting surface. Below are the polar and rectangular plots that shows on comparing MTPO and PO.
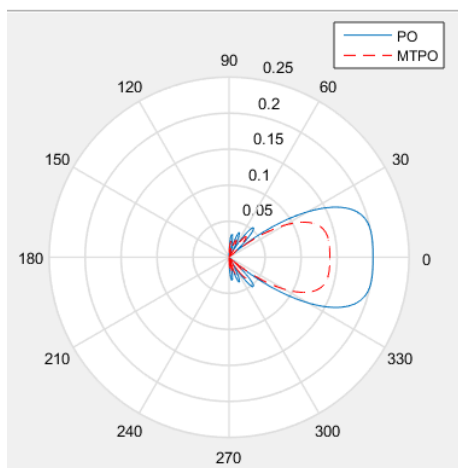
Fig.8 Comparism between MTPO and PO
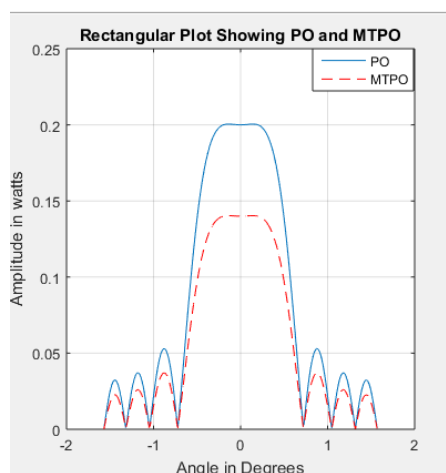
Fig.9 Rectangular plot showing MTPO and PO.

Using Polar plot.

Table 3 Difference in dB between MTPO and PO main and side lobes

S/N	LOBE	PO IN dB	MTPO in dB	DIFFERENCE IN dB
1	Main Lobe	-7	-9	2
2	First Side Lobe	-13	-14	1
3	Second Side Lobe	-14	-16	2
4	Third Side Lobe	-15	-16	1

From table 3, the difference between the main lobe of MTPO and PO is 2dB while the difference between the three side lobes of MTPO and PO are 1dB, 2dB and 1dB respectively. The difference is dependent on the distance (d).

For beam width, rectangular and polar plot were used to analyse the 3dB or half power beam width (HPBW) of both MTPO and PO radiation pattern respectively. Both equation 45 for MTPO and equation 28 for PO were plotted with the following values $\varphi = (-\pi/2, 0.01, \pi/2)$, $\lambda = 3m$ and n=4. The HPBW is traced from the gain axis against the angle in degrees. The rectangular and polar plots of MTPO, PO and both MTPO and PO combined are shown below
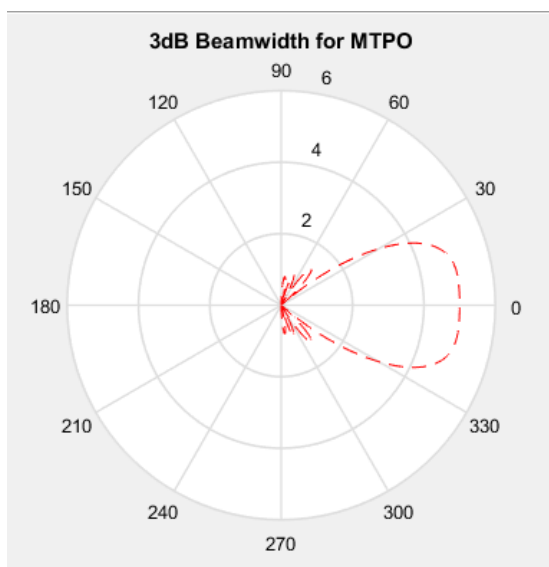
Fig.10Polar plot showing 3dB
Beam width of MTPO.
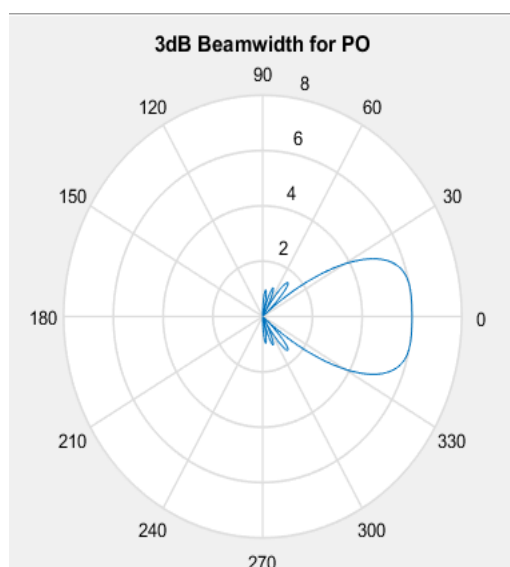
Fig.11 Polar plot showing 3dB
Beam width of PO.
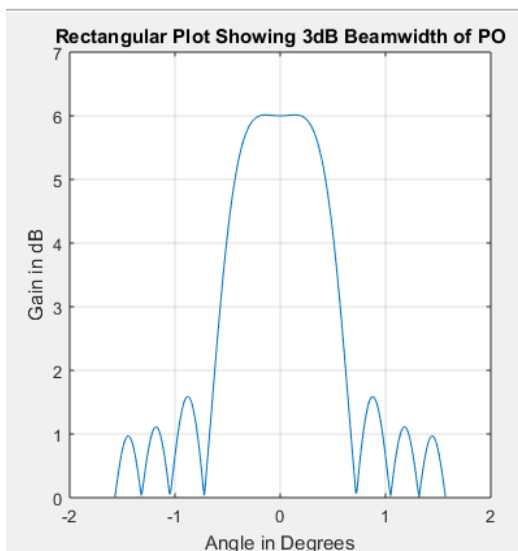
Fig. 12 Rectangular plot showing the 3dB beam width of PO.
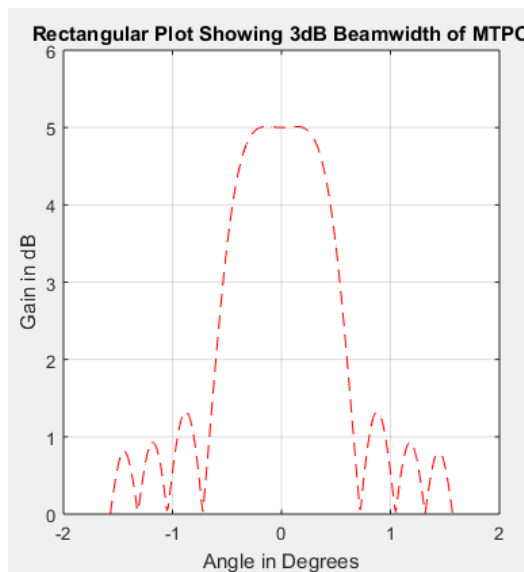
Fig. 13 Rectangular plot showing the 3dB beam width of MTPO.
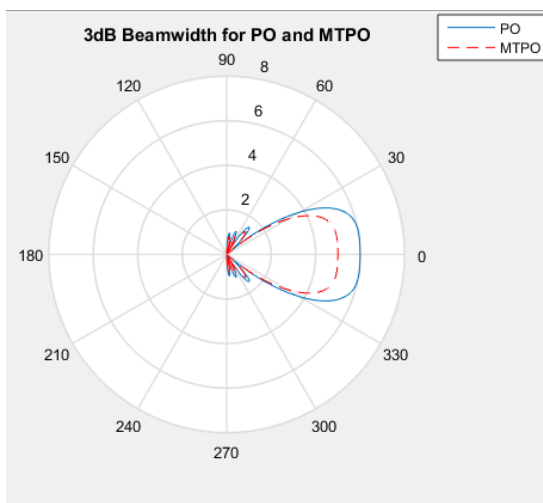
Fig.14 Polar plot showing 3dB Beam width of MTPO and PO.
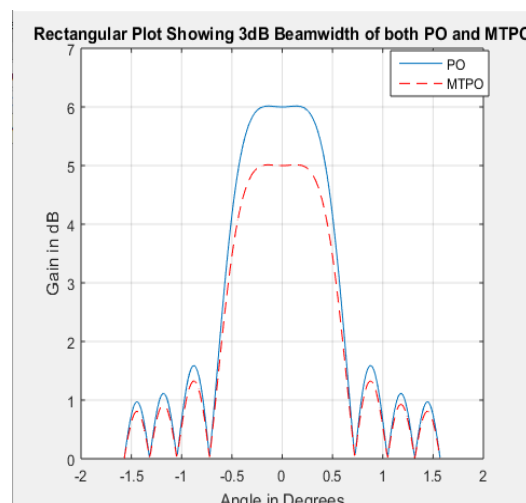
Fig.15 Rectangular plot showing 3dB Beam width of PO and MTPO.

From figures 10 to 15, it shows that MTPO beam width is narrower than that of PO. Although the field strength of PO is higher than that of MTPO, PO radiation pattern will perform better in long distance communication provided that the side lobe radiations are minimized. The narrower beam width of MTPO increases the directivity, efficiency and signal to noise ratio (SNR), making it possible to be applied in satellite communication.

V.   Conclusion

In this paper, edge diffraction was reduced in parabolic antenna used for satellite communication. This was possible because of MTPO employed Stationery Point Method and Edge Point Techniqueto evaluate scattered and diffracted field at the edge of parabolic reflector. From the simulation using Mathlab, it was discovered that diffracted field at the edge showed itself as side lobes (more) which depends on distance. A comparism between MTPO and PO using both mathematical and physical observation method showed that PO has more side lobes than MTPO. The reduction of side lobes by MTPO was because of introduction of aperture surface (second surface). This MTPO has three axioms that it uses to obtain scattering integral, which makes it possible for MTPO to solve scattering problem on different surfaces such as half plane, impedance half plane, PEC cylindrical reflector and impedance reflector surface.

References

[1]. Dandu, .O. (2013). *Optimized design of axially symmetrical cassegrain reflector antenna using iterative local search algorithm*. A Published M.Tech project of National Institute of Technology.

[2]. Yahya, R.S & Rand, (2015). *Reflector antenna developments a prospective on the past, present and future*. An IEEE antennas and propagation magazine, 57 (2).

[3]. Biebuma, J.J (2017). *Radio propagation for mobile communication*. Net code Research and printing house Choba, Port Harcourt. ISBN: 978-978-54815-5-2.

[4]. Turk A.S (2005).*Analysis of aperture illumination and edge rolling effects for parabolic reflector antenna design*. International Journal of Electronics and communication ACU 60(2006), 257-266.

[5]. Lorenzo, J.A.M, Pino, A.G, Vega, .I, Arias, .M. &Rubinos, (2005).*Induced current analysis of reflector antenna (ICARA)*. IEEE Antenna and Propagation Magazine 47 (2).

[6]. Wu, .Y.M & Chew, W.C (2016). *The modern high frequency methods for solving electromagnetic scattering problems*. Progress on Electromagnetic Research,156,63-82.

[7]. Umul, Y.Z (2009).*Rigorous expressions for the equivalent edge current*. Progress on Electromagnetic research, 156, 63-82.

[8]. Miller, .K. &Krentel, R.W. *Analysis of compact range reflectors with serrated edge*. A Publication of Semanticscholar.org, Corpus ID: 173988174.

[9]. Kilic, .G. (2016).*Radiation from parabolic type radio link antennas*. A Published M.sc Thesis, Cankaya University Turkey.

[10]. Umul, Y.Z, (2004). *Modified Theory of Physical Optics*. Optical Society of America (OSA),12 (20), Optics Express 4959.

[11]. Dinc, .G. (2014).*Line integral representation of fringe wave for perfectly conducting and impedance Surfaces*. A Published M.Sc Thesis of Cankaya University Turkey.

[12]. Umul, Y.Z. (2008).*Scattering of a line source by a cylindrical parabolic impedance surface.* A Journal of Optic Society AM, 25(7), 1625-1659.

[13]. Sarnik, .M. (2015). *Analysis of the scattering field from PEC curved surfaces with MTPO.* An Unpublished M.Sc Thesis of Dept. Of Elect/Elect. Eng. Of Uludag University Turkey.

[14]. Okerulu, C.I. (2020).*Minimizing edge diffraction in parabolic antenna for satellite communication.* An unpublished M.eng Thesis of Elect./Elect.Eng, University of Port Harcourt Rivers State, Nigeria.

[15]. Sarnik, .M. &Yacin,.U. (2010).*Calculation of diffraction of the uniform fields from a black half plane by Physical Optics Method*.Cankaya University Journal Science Engineering, 7(2), 95-104.

[16]. Umul, Y.Z. (2005).*Diffraction by a black half plane: Modified Theory of Physical Optics approach*. Optics express, 13(19), 7276-7287.

[17]. Yacin, .U. &Sarnik .M. (2013).*Uniform diffracted fields from a perfectly conducting reflector with Modified Theory of Physical Optics*.Science World Journal, Article ID: 195402.

[18]. Basdemir, H.D (2013).*Impedance surface diffraction analysis for a strip with the boundary diffraction wave theory*. Optic International Journal of light electron opt, 627-630.

[19]. Yacin .U. (2009).*Uniform scattered fields of the extended theory of boundary diffraction wave for PEC surfaces programme electromagnetic*. RCS M7, 29-39.